Contrib Mineral Petrol (1993) 114:63–78

Contributions to Mineralogy and Petrology

Multiphase inclusions in plagioclase from anorthosites in the Stillwater Complex, Montana: implications for the origin of the anorthosites

Patricia J. Loferski[1] **and Richard J. Arculus**[2]

[1] US Geological Survey, M.S. 954, Reston, VA 22092, USA
[2] Department of Geology and Geophysics, University of New England, Armidale, NSW 2351, Australia

Received March 16, 1992 / Accepted November 24, 1992

Abstract. Multiphase inclusions, consisting of clinopyroxene + ilmenite + apatite, occur within cumulus plagioclase grains from anorthosites in the Stillwater Complex, Montana, and in other rocks from the Middle Banded series of the intrusion. The textures and constant modal mineralogy of the inclusions indicate that they were incorporated in the plagioclase as liquid droplets that later crystallized rather than as solid aggregates. Their unusual assemblage, including a distinctive manganiferous ilmenite and the presence of baddeleyite (ZrO_2), indicates formation from an unusual liquid. A process involving silicate liquid immiscibility is proposed, whereby small globules of a liquid enriched in Mg, Fe, Ca, Ti, P, REE, Zr and Mn exsolved from the main liquid that gave rise to the anorthosites, became trapped in the plagioclase, and later crystallized to form the inclusions. The immiscibility could have occurred locally within compositional boundaries around crystallizing plagioclase grains or it could have occurred pervasively throughout the liquid. It is proposed that the two immiscible liquids were analogous, in terms of their melt structures, to immiscible liquid pairs reported in the literature both in experiments and in natural basalts. For the previously reported pairs, immiscibility is between a highly polymerized liquid, typically granitic in composition, and a depolymerized liquid, typically ferrobasaltic in composition. In the case of the anorthosites, the depolymerized liquid is represented by the inclusions, and the other liquid was a highly polymerized aluminosilicate melt with a high normative plagioclase content from which the bulk of the anorthosites crystallized. Crystallization of the anorthosites from this highly polymerized liquid accounts for various distinctive textural and chemical features of the anorthosites compared to other rocks in the Stillwater Complex. A lack of correlation between P contents and chondrite-normalized rare earth element (REE) ratios of plagioclase separates indicates that the amount of apatite in the inclusions is too low to affect the REE signature of the plagioclase separates. Nevertheless, workers should use caution when attempting REE modelling studies of cumulates having low REE contents, because apatite-bearing inclusions can potentially cause problems.

Correspondence to: P.J. Loferski

Introduction

One of the enigmatic aspects of the Stillwater Complex, Montana is the origin of two massive sheets of anorthosite, each several hundred meters thick, within the Middle Banded series. Since first investigated by Hess (1960), the Stillwater anorthosites have been the focus of a variety of studies (Raedeke 1982; Salpas et al. 1983; Scheidle 1983; Czamanske and Scheidle 1985; Czamanske and Bohlen 1990; Haskin and Salpas 1992), but their origin and relation to the rest of the Stillwater Complex remain controversial. Some of the enigmatic aspects of the anorthosites, known as Anorthosite zones I and II (AN I and AN II), include not only their extremely plagioclase-rich compositions (typically 85 to 95% plagioclase) but also the occurrence of plagioclase as the only cumulus mineral over hundreds of stratigraphic meters, their association with rocks that contain cumulus Mg-rich olivine after its absence for about 1000 stratigraphic meters, and their association with rocks that display a different crystallization sequence (plagioclase-olivine-clinopyroxene-orthopyroxene) than most of the underlying parts of the Stillwater Complex (olivine-orthopyroxene-plagioclase-clinopyroxene) (Raedeke and McCallum 1980). It is difficult to explain these features by normal fractionation of a single basaltic magma type.

Studies of the Stillwater Complex have led to hypotheses that it formed through the intrusion of two different parental magma types rather than from a single parental magma (Todd et al. 1982; Irvine et al. 1983). Irvine et al. (1983) hypothesized that the anorthosites formed from the second magma type, possibly a high-alumina basalt having plagioclase on the liquidus, which they referred to as the anorthositic, or A-type magma. They hypothe-

sized that most of the rest of the Stillwater Complex formed from a boninite-like magma having orthopyroxene on the liquidus, which they referred to as the ultramafic or U-type magma.

In addition to two-liquid hypotheses, other models for the origin of the anorthosites include (1) physical concentration of liquid enriched in plagioclase components through resorption, convection, and reprecipitation (Hess 1960); (2) mixing of a fresh and a differentiated magma, producing a hybrid melt within the primary liquidus volume of plagioclase (Irvine 1975); (3) crystallization of plagioclase from the same liquid as underlying parts of the complex in a pressure gradient followed by coalescence of large anorthositic "rockburgs" (Raedeke and McCallum 1980; McCallum et al. 1980; Raedeke 1982); and most recently (4) intrusion of sills of crystal-laden anorthositic mush that originated in a deep staging chamber from which other Stillwater magmas may have been derived (Czamanske and Bohlen 1990).

Rare earth element (REE) geochemical studies can be extremely useful in constraining models for the origin of the Stillwater Complex in general and the anorthosites in particular. Especially powerful are studies of the REE geochemistry of plagioclase separates. Prior to such REE geochemical studies it is crucial to accurately identify and understand the mineralogic hosts of these elements within the rocks. The present study documents the presence of multiphase apatite-bearing inclusions in cumulus plagioclase from the Stillwater anorthosites and other rocks from the Middle Banded series. The apatite within the inclusions may have important implications for REE modelling because of the high mineral/melt partition coefficients for apatite (Hanson 1980). In addition, the proposed origin of the inclusions as an immiscible liquid has implications for the physical and chemical nature of the parent liquid of the anorthosites.

General geology

The Stillwater Complex is an Archean stratiform mafic and ultramafic intrusion that crops out for a strike-length of about 48 km along the northern front of the Beartooth Mountains of southwestern Montana. Various isotopic studies, the most recent by Premo et al. (1990), indicate a crystallization age of about 2700 Ma. The Stillwater Complex was intruded into Middle Archean metasedimentary rocks and is overlain unconformably by Paleozoic and Mesozoic sedimentary rocks. It was tilted during the Laramide orogeny, and its layering now dips steeply to the northeast and is locally vertical to overturned. Various aspects of the geology and ore deposits of the Stillwater Complex are reported by Czamanske and Zientek (1985 and references therein).

Following the stratigraphic nomenclature of McCallum et al. (1980), modified by Zientek et al. (1985), the Stillwater Complex is subdivided into the following major units (Fig. 1): (1) a Basal series, which is as much as about 240 m thick and consists of bronzite-rich cumulates and minor segregations of noncumulate rocks, (2) an Ultramafic series, which averages about 1000 m thick and is composed of cumulates of olivine, bronzite, and chromite, and (3) the Lower, Middle, and Upper Banded series, totalling about 4500 m in thickness and consisting of cumulates of plagioclase, augite, bronzite, and olivine.

The Middle Banded series is anomalously rich in plagioclase, containing an estimated 82 vol.% through its 1700-m thickness

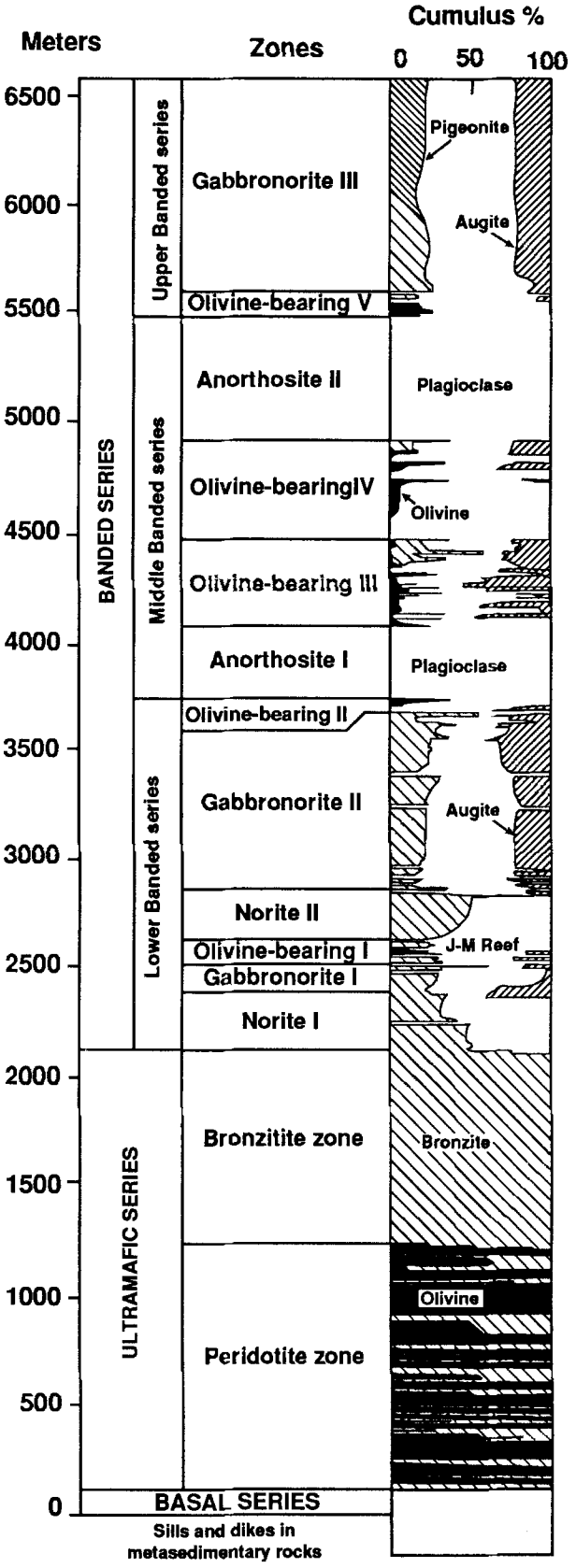

Fig. 1. Stratigraphic column of the Stillwater Complex, showing the cumulus mineralogy, from Boudreau and McCallum (1989) as modified after McCallum et al. (1980) and Zientek et al. (1985)

(McCallum et al. 1980). AN I and AN II are the thickest anorthosites in the Middle Banded series. Both layers vary in thickness along strike up to a maximum of about 350 m for AN I and 570 m for AN II. The anorthosites are separated by about 700 m of complexly interlayered plagioclase-olivine, plagioclase-augite, plagioclase-olivine-augite, and plagioclase-olivine-augite-bronzite cumulates. In addition, other thin anorthosite layers occur between AN I and AN II, and a third thick anorthosite layer, approximately 100 m thick, occurs at the base of Olivine-bearing zone IV (Fig. 1).

Characteristics of the anorthosites

Detailed descriptions of the mineralogy, textures and field relations of AN I and AN II have been given by Hess (1960), McCallum et al. (1980), Scheidle (1983) and Czamanske and Scheidle (1985). In brief, the average composition of plagioclase is approximately the same in AN I, AN II and the cumulates between them, about An_{75} to An_{77}, and there is no evidence of systematic change in composition with stratigraphic position. Within AN I and AN II, however, individual plagioclase grains are complexly zoned, and have compositional variations of as much as 12 mol% An. Grains showing normal, reverse and oscillatory zoning patterns are found within single thin sections.

Clinopyroxene and inverted pigeonite are the typical intercumulus minerals, and they exhibit two different textures on an outcrop scale. In some places they form discrete oikocrysts, from 2 to 10 cm across, but in most places the pyroxene forms extensive interconnected networks.

AN I and AN II are texturally distinctive because many plagioclase grains are two to three times larger than cumulus plagioclase from other zones in the complex (Hess 1960; McCallum et al. 1980; Scheidle 1983; Foose 1985). Grain size within these thick anorthosites ranges from 4 to 15 mm with an average length of about 6 mm (Scheidle 1983). Finer-grained facies, in which plagioclase crystals average about 2 mm in length, occur locally along the lower contacts of both AN I and AN II as well in a distinctive 5- to 15-m-thick zone at the top of AN II. Lamination occurs locally in these finer grained zones, but there is no other discernible foliation or modal layering in the anorthosites. In contrast, lamination is common in other plagioclase-bearing cumulates within the Banded series, including thin layers of anorthosite. The massive, unlaminated texture of AN I and AN II must be accounted for when considering their origin.

Methods

Approximately 160 samples were collected from AN I, AN II and surrounding units along traverses normal to the layering at several locations across the complex. Polished thin sections of the samples were examined in transmitted and reflected light. The compositions of plagioclase, pyroxene, ilmenite, and apatite were determined by electron microprobe analysis of one to three or more points per grain, depending on grain size. The analyses were performed on the ARL- SEMQ electron microprobe at the US Geological Survey, Reston. Standard operating conditions utilized an accelerating potential of 15 kV and a beam current of 100 nanoamps. The analyses were performed with a focused beam spot, except for intercumulus clinopyroxene, which was analyzed with a 10-μm beam spot in order to include orthopyroxene exsolution lamellae. Data were reduced by using the method of Bence and Albee (1968). Three samples were selected for detailed study with a scanning electron microscope. Analyses for P by inductively coupled plasma source spectroscopy (ICP) and REE by instrumental neutron activation analysis (INAA) of plagioclase separates were obtained at the analytical laboratories of the US Geological Survey. ICP spectroscopy has a detection limit of 1 ppm for P and a precision of ±5 to 10% for concentrations of 5–50 ppm, which covers the range found in our samples.

Petrography

General features of the anorthosites

Within individual samples, the plagioclase grains typically form an interconnected network. The grains range from lath shaped to equant and from subhedral to anhedral. Some have smooth grain boundaries, whereas others have ragged and/or sutured boundaries. The zoning that occurs in much of the plagioclase can be detected optically by differences in the extinction angles. The zones are broad and diffuse, typically 100 to 500 μm across, possibly as a result of slow cooling.

Intercumulus clinopyroxene and inverted pigeonite typically compose from 10 to 15 modal % of individual samples but range from traces to about 20 modal %. The intercumulus clinopyroxene contains exsolution lamellae of orthopyroxene, and the inverted pigeonite contains blebs and lamellae of clinopyroxene. Other intercumulus phases observed in this study include quartz, ilmenite, and sulfide minerals. Quartz contains minute fluid inclusions, and in some samples it is oikocrystic. Ilmenite occurs as rare, small grains, which typically occur at the grain boundaries between plagioclase and intercumulus pyroxene. Pyrrhotite and chalcopyrite, with minor pentlandite, occur in small patches and are associated with epidote and other low-temperature alteration products. No intercumulus apatite was noted in this study, but it has been reported to occur in the anorthosites (Boudreau and McCallum 1986).

Some anorthosite samples and some areas within individual thin sections are virtually free of intercumulus phases. In these areas, plagioclase grains are smaller and more equant than those in other samples, they do not appear to be zoned, and many exhibit 120° triple-grain junctions. Samples exhibiting this annealed texture are randomly distributed in both AN I and AN II.

Some of the samples are fresh, but many are altered to various degrees. The pyroxenes are typically the first minerals to become altered, and it is not unusual to find altered pyroxene coexisting with fresh plagioclase in a thin section. Pyroxene alteration products include serpentine and chlorite; plagioclase is altered to sericite and epidote. One sample (82PPC7) from the Picket Pin Mountain traverse of AN II contains intercumulus olivine. Olivine is rare in the anorthosites and has been reported to occur only near the Picket Pin platinum group element (PGE)-bearing zone near the top of AN II (Boudreau and McCallum 1986). Because our sample is from approximately 200 m below the Picket Pin PGE zone, a more widespread occurrence of intercumulus olivine in AN II is indicated.

Multiphase inclusions

Figure 2a shows a cumulus plagioclase grain that contains a typical small multiphase inclusion. The inclusion consists of clinopyroxene + ilmenite + apatite. Such inclusions were found in all of the anorthosite samples that were studied, as well as in samples from other units in the Middle Banded series, but were not found in the few samples studied from the Lower and Upper Banded series.

Most of the inclusions are 50–150 μm across, but some are as much as several hundred μm across. The apatite grains in the inclusions range in diameter from about 2 μm in the smallest inclusions to about 30 μm in the largest inclusions; most are less than 10 μm across. The inclusions are randomly distributed within samples and vary in abundance from sample to sample. In any given sample some plagioclase grains are free of inclusions, some grains contain one, and others contain several (Fig. 2b). Most inclusions occur within the interiors

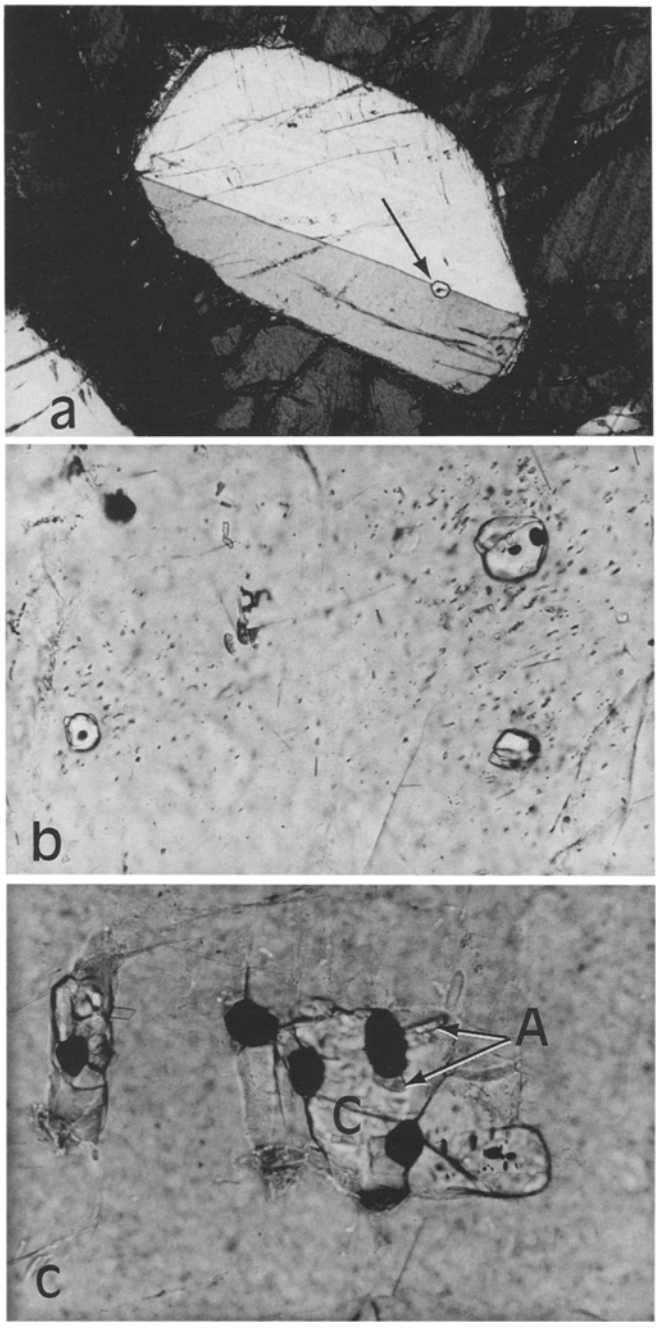

Fig. 2a–c. Photomicrographs taken in transmitted light of multiphase inclusions in plagioclase from the Stillwater anorthosites. **a** Multiphase inclusion (*arrow*) on twin plane of plagioclase host. Field of view, 3 mm across; **b** Group of three inclusions in plagioclase, each containing a single grain of clinopyroxene and either single or multiple grains of ilmenite (black) and apatite; field of view, 700 μm across; **c** Large inclusions containing multiple grains of clinopyroxene (*C*), ilmenite (black) and apatite (*A*); field of view = 700 μm across

of plagioclase grains and are not related to fractures within the grains. The inclusions display a variety of shapes. Many are rounded, whereas others are elongate and have length-to-width ratios of 4:1 or 5:1. Some, such as the one shown in Fig. 2a, occur along twin planes in the plagioclase host. Visual estimates for hundreds of the inclusions, using the determinative charts of Terry and Chillenger (1955), show that individual inclusions consist of about 5 to 15% ilmenite and 2 to 5% apatite, with the remainder being a combination of clinopyroxene plus plagioclase that crystallized along the inclusion walls.

Most of the inclusions are composed of a single clinopyroxene grain that encloses either single or multiple grains of ilmenite and apatite. The larger inclusions consist of multiple grains of all three phases and commonly display 120° triple-junctions between the clinopyroxene grains, possibly as a result of prolonged annealing postdating the complete solidification of the inclusions (Fig. 2c). Many of the inclusions are unaltered, but in some, the ilmenite is rimmed and embayed by sphene ± rutile, and some of the clinopyroxene is altered to talc. Reflected-light optical examination and scanning electron microscopy reveal angular voids in many of the inclusions. Some of these voids may be mineral fragments that were plucked out, whereas other voids probably formed as a result of contraction of the inclusions upon cooling. In addition to the phases described, one multiphase inclusion contained a spherical bleb of sulfide that energy dispersive analysis shows to contain Cu, Ni and Fe. Thin rims of calcic plagioclase (as high as An_{92}) are optically detectable around the largest inclusions by a difference in extinction angle compared with the host plagioclase. These zones are commonly less than 5 μm wide but can be as much as 8 μm wide.

Scanning electron microscopy of three samples shows that baddeleyite (ZrO_2) occurs in many of the inclusions. The baddeleyite grains are typically less than 1 μm across, and most are associated with the ilmenite, forming either single lamellar inclusions or small blebs at ilmenite grain boundaries, a texture suggestive of granule exsolution. Baddeleyite was originally thought to be restricted to lunar basalts and undersaturated terrestrial igneous rocks, in which the activity of SiO_2 was below the level at which zircon would form by the reaction: $ZrO_2 + SiO_2 = ZrSiO_4$. The texture of the baddeleyite in the Stillwater inclusions, however, implies that it exsolved from the ilmenite. Therefore, low silica activity of the melt from which the inclusions formed cannot be inferred. The only other reported occurrence of badelleyite in the Stillwater Complex is in the vicinity of the PGE-bearing J-M Reef in Olivine-bearing zone I (Premo et al. 1990). Baddeleyite has recently been found in association with ilmenite in tholeiitic rocks, including the Basistoppen Sill, associated with the Skaergaard intrusion (Naslund 1987), and in the Skaergaard intrusion itself (Kersting et al. 1989).

In addition to the multiphase inclusions, the plagioclase in the Stillwater anorthosites also contains ilmenite rods (identified by energy dispersive analysis), which are crystallographically oriented in the plagioclase host.

Mineral chemistry

Pyroxene

Representative electron microprobe analyses of intercumulus and inclusion clinopyroxene are listed in Table

Table 1. Representative electron microprobe analyses of clinopyroxene

	82PPC5			82PPC9		
	Int[a]	Incl[b]	Incl	Int	Incl	Incl
SiO_2	52.21	52.18	53.10	51.09	50.91	51.11
TiO_2	0.35	0.34	0.18	0.40	0.47	0.23
Al_2O_3	1.68	1.53	0.83	1.64	1.79	1.05
Cr_2O_3	0.04	0.01	0.04	0.07	0.01	0.07
Fe_2O_3[c]	0.06	0.39	0.00	0.00	1.94	2.21
FeO	8.58	7.65	6.39	9.62	7.66	9.11
MnO	0.14	0.10	0.04	0.26	0.25	0.25
MgO	14.76	15.03	15.14	14.61	14.03	13.25
CaO	21.09	21.47	22.85	21.04	21.64	21.61
Na_2O	0.15	0.14	0.11	0.26	0.14	0.14
Total	99.06	98.84	98.68	98.99	98.84	99.03
Cations based on six oxygens						
Si	1.96	1.96	1.98	1.93	1.92	1.94
AlIV	0.04	0.04	0.02	0.07	0.08	0.05
AlVI	0.03	0.02	0.02	0.01	0.00	0.00
Ti	0.01	0.01	0.01	0.01	0.01	0.01
Cr	0.00	0.00	0.00	0.00	0.00	0.00
Fe^{+3}	0.00	0.01	0.00	0.00	0.06	0.06
Fe^{+2}	0.27	0.24	0.20	0.30	0.24	0.29
Mn	0.00	0.00	0.00	0.01	0.01	0.01
Mg	0.82	0.84	0.84	0.82	0.79	0.75
Ca	0.85	0.86	0.92	0.85	0.88	0.88
Na	0.01	0.01	0.01	0.02	0.01	0.01
Wo	44	44	47	43	46	46
En	42	43	43	42	41	39
Fs	14	13	10	15	13	15

[a] Int, intercumulus
[b] Incl, inclusion
[c] Fe_2O_3 calculated

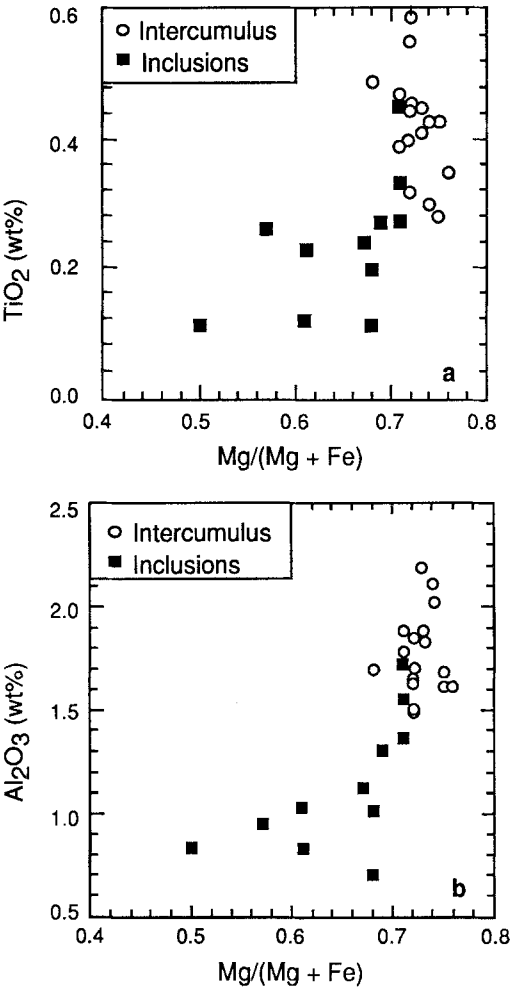

Fig. 3. **a** Plots of TiO_2 and **b** Al_2O_3 versus X_{Mg} for intercumulus and inclusion clinopyroxene

1. The bulk of the clinopyroxene in the inclusions overlaps in composition with the intercumulus clinopyroxene in terms of $Mg/(Mg+Fe^{2+})$, or X_{Mg}, with values generally between 0.70 and 0.75. Clinopyroxene in a few inclusions is more Fe-rich, with X_{Mg} values as low as 0.50. No correlation was apparent between X_{Mg} of the clinopyroxene and the distance of the inclusion from the rim of the host plagioclase grain.

Scanning electron microscopy revealed that the clinopyroxene in the inclusions does not contain detectable orthopyroxene lamellae. In contrast, the intercumulus pyroxenes are similar to pyroxenes from tholeiitic rocks; that is, there are two pyroxenes, and each contains exsolution lamellae of the other. Intercumulus host and guest inverted pigeonite pairs plot near the 600° C, 10^5 Pa isotherm on the pyroxene quadrilateral of Lindsley (1983). This temperature is presumably that at which microscopically-visible exsolution ceased.

Plots of Al_2O_3 and TiO_2 against X_{Mg} for intercumulus and inclusion clinopyroxene in one representative sample are shown in Fig. 3. The two types of clinopyroxene occupy distinct, but partially overlapping, compositional fields. The inclusion clinopyroxene extends to lower Al_2O_3 and TiO_2 values and, in this sample, lower X_{Mg}. Other samples show overlapping to slightly higher X_{Mg} in the inclusions. MnO contents in both the inclusion and intercumulus clinopyroxene are about 0.1 to 0.3 wt.%; Cr_2O_3 concentrations are negligible, generally less than 0.05 wt.%.

Ilmenite

Representative electron microprobe analyses of ilmenite are listed in Table 2, which includes both intercumulus grains and those within multiphase inclusions. The ilmenites have notably high MnO contents, typically greater than 1 wt.% MnO; ilmenite in the inclusions contains as much as 7.5 wt.% MnO (Fig. 4). Within individual samples, ilmenite grains in the inclusions generally have higher MnO contents than intercumulus ilmenite grains. Published analyses of ilmenite from other mafic layered intrusions, including the Bushveld Complex (South Africa), Skaergaard Intrusion (East Greenland), Duluth Complex (Minnesota), Kiglapait Intrusion (Labrador), and the Glen Mountains Layered Complex (Oklahoma), show less than about 1 wt.% and commonly less than 0.05 wt.% MnO (Wager and Brown 1968;

Table 2. Representative electron microprobe analyses of ilmenite

	82PPC7		82PPC9		84CML1	
	Int[a]	Incl[b]	Int	Incl	Int	Incl
SiO_2	0.03	0.02	0.07	0.01	0.08	0.05
TiO_2	48.22	50.82	49.07	50.17	49.08	51.55
Al_2O_3	0.00	0.00	0.00	0.00	0.00	0.00
Cr_2O_3	0.04	0.02	0.04	0.00	0.04	0.02
Fe_2O_3	0.00	0.00	0.00	0.00	0.00	0.00
FeO	45.63	40.23	45.98	39.53	47.18	44.76
MnO	3.07	6.43	2.44	7.43	1.29	1.42
MgO	0.06	0.16	0.07	0.01	0.06	0.09
CaO	0.42	0.06	0.08	0.56	0.08	0.22
Total	97.47	97.74	97.75	97.71	97.81	98.11
Cations based on three oxygens						
Si	0.00	0.00	0.00	0.00	0.00	0.00
Ti	0.93	0.98	0.95	0.97	0.95	1.00
Al	0.00	0.00	0.00	0.00	0.00	0.00
Cr	0.00	0.00	0.00	0.00	0.00	0.00
Fe^{+3}	0.13	0.03	0.10	0.05	0.10	0.00
Fe^{+2}	0.85	0.84	0.89	0.79	0.92	0.96
Mn	0.07	0.14	0.05	0.16	0.03	0.03
Mg	0.00	0.01	0.00	0.00	0.00	0.00
Ca	0.01	0.00	0.00	0.02	0.00	0.01

[a] Int, intercumulus
[b] Incl, inclusion

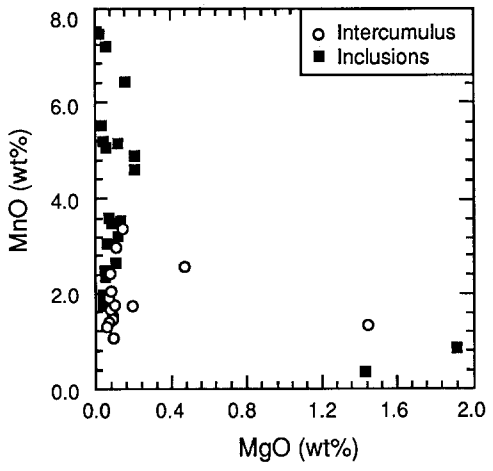

Fig. 4. Plot of MnO versus MgO for intercumulus and inclusion ilmenite showing the manganiferous nature of some of the inclusion ilmenite

Morse 1980; Pasteris 1985; Reynolds 1985; Scofield and Roggenthen 1986). The manganiferous nature of the Stillwater ilmenites is therefore unusual for intrusive mafic rocks.

Bacon and Hirschmann (1988) suggested that high MnO ilmenites in intrusive rocks may result from late-stage enrichment due to Mn migration, possibly in an aqueous phase, during open-system slow cooling. In the Stillwater anorthosites, however, late stage Mn enrichment of the inclusion ilmenite is unlikely because the grains are enclosed within plagioclase and would have been isolated from late magmatic-hydrothermal fluids.

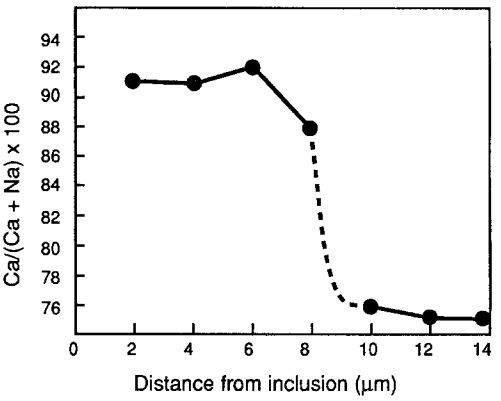

Fig. 5. Plot of a microprobe traverse in plagioclase showing change in the An content near a multiphase inclusion

Therefore, it is more likely that the Stillwater inclusion ilmenites acquired their high MnO contents by crystallization from a MnO-rich liquid.

Plagioclase

An electron microprobe traverse across a particularly wide calcic zone surrounding a large (>200 μm diameter) inclusion is shown in Fig. 5. The An content of plagioclase is highest near the clinopyroxene in the inclusion (An_{92}), and ranges from An_{75} to An_{80} throughout the rest of the grain. The calcic rims on other inclusions have compositions of An_{88} to An_{91}. The rims are typically several μm wide and are interpreted as being cognate to the inclusion. Calcic plagioclase rims are not analytically or optically resolvable on smaller (<200-μm-wide) inclusions.

Apatite

It is difficult to obtain electron microprobe analyses of the apatite in the inclusions because, of the few grains that are exposed at the surfaces of thin sections, most are less than 10 μm across. Apatite compositions for three samples are shown in Table 3. The samples include two anorthosites from AN II (82PPC7 and 82PPC9), one of which contains intercumulus olivine (82PPC7), and a plagioclase-augite-olivine cumulate from Olivine-bearing zone III (84CML1).

Apatite compositions are shown plotted with respect to F, Cl, and OH in Fig. 6. Also included are data from Boudreau (1986) and Boudreau and McCallum (1989) for intercumulus apatite from the Banded series. Each sample from the present study plots in a discrete field. Anorthosite sample 82PPC9 contains F-rich apatite, with as much as 3.2 wt.% F, whereas anorthosite sample 82PPC7 contains relatively Cl-rich apatite, with as much as 2.7 wt.% Cl. The plagioclase-augite-olivine cumulate contains Cl-rich apatite, with as much as 3.5 wt.% Cl.

Most igneous apatite is F-rich and typically contains less than 1 wt.% Cl (Nash 1984). The Cl-rich apatite in the Stillwater Complex is therefore unusual. Boudreau

Table 3. Representative electron microprobe analyses of apatite in inclusions

	82PPC7		82PPC9		84CML1	
Grain:	1	2	1	2	1	2
CaO	54.15	53.85	54.91	55.21	54.52	54.96
P_2O_5	40.08	39.78	41.07	40.23	40.52	40.77
FeO	0.54	0.52	0.76	0.60	0.23	0.31
MgO	0.02	0.05	0.13	0.04	0.10	0.05
SiO_2	0.37	0.54	0.48	0.29	0.33	0.26
Ce_2O_3	0.19	0.27	0.06	0.09	0.04	0.35
F	1.15	1.27	3.19	2.89	0.84	0.90
Cl	2.74	2.93	0.63	1.11	3.48	3.09
Total	99.24	99.21	101.23	100.46	100.06	100.69
$O \equiv F$, Cl	1.11	1.20	1.48	1.47	1.15	1.09
Total	98.13	98.01	99.75	98.99	98.91	99.60
F/(F+Cl+OH)	0.33	0.36	0.88	0.78	0.24	0.25
Cl/(F+Cl+OH)	0.42	0.45	0.09	0.16	0.53	0.47
OH/(F+Cl+OH)	0.25	0.19	0.03	0.06	1.23	0.28

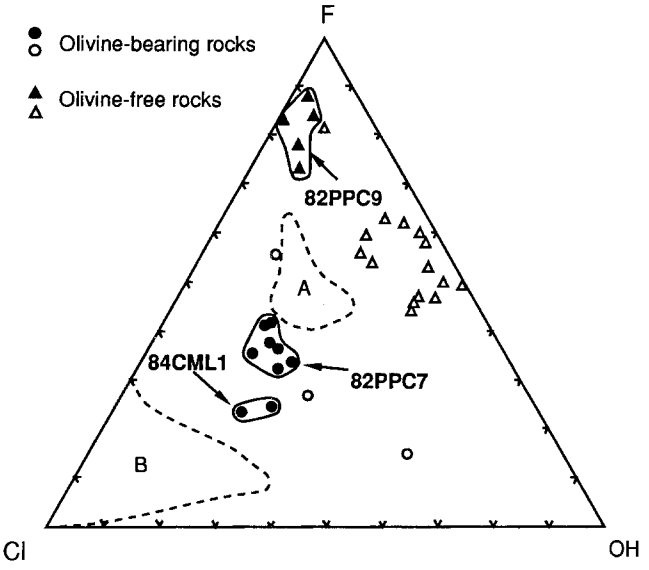

Fig. 6. Compositions of apatite plotted with respect to F−Cl−OH. *Filled symbols* are apatites within multiphase inclusions from this study, *open symbols* as well as fields *A* and *B* are data for intercumulus apatite from Boudreau (1986) and Boudreau and McCallum (1989): *A*, olivine-bearing rocks from Olivine-bearing zone I; *B*, anorthosites and norites from Olivine-bearing zone I

and McCallum (1989) found extremely Cl-rich apatite, containing as much as 7 wt.% Cl and virtually no F, throughout the lower third of the Stillwater Complex, including the Ultramafic series and the lowermost part of the Lower Banded series. They found that more F-rich apatite, containing as much as 1.6 wt.% F and 2.3 wt.% Cl, first occurs within Olivine-bearing zone I, just below the J-M Reef. Cl-apatite also occurs in Norite II, but above this zone, Cl contents generally decrease, although apatite with as much as 3 wt.% Cl does occur in many samples.

The Stillwater Cl-rich apatite is associated with olivine-bearing rocks in the three samples analyzed here and in many of the samples from Olivine-bearing zone I and the Middle Banded series analyzed by Boudreau (1986) and Boudreau and McCallum (1989). As shown in Fig. 6, apatite from olivine-bearing rocks from these zones (including our intercumulus olivine-bearing anorthosite sample 82PPC7) has $Cl/(Cl+F+OH) > 0.28$, and apatite from olivine-free rocks has $Cl/(Cl+F+OH) < 0.4$.

The origin of the Cl-rich apatite is debatable. Boudreau and McCallum (1989) attributed the extremely Cl-rich apatite in the lower third of the Stillwater Complex to a process they called vapor-driven constitutional zone refining. Through this process, a vapor phase, into which Cl was partitioned relative to F, was hypothesized to have exsolved from the intercumulus melt, migrated upward through the cumulate pile, and redissolved in hotter interstitial melts higher in the complex. This resulted in an increase in the Cl/F ratio of both the intercumulus melt and phases such as apatite that eventually crystallized from that melt. Degassing at the top of the magma chamber was proposed to have caused an overall loss of Cl, resulting in the more F-rich intercumulus apatites stratigraphically higher in the Stillwater Complex. The association of Cl-rich apatite with both of the PGE zones, the J-M Reef and the Picket Pin zone, has been cited as one line of evidence that the PGE were transported and deposited from Cl-rich fluids during a late magmatic-hydrothermal event (Boudreau et al. 1986).

Although it is possible that a process such as vapor-driven constitutional zone refining did occur and may have affected the intercumulus apatite, it does not account for the association of Cl-rich apatite with olivine-bearing rocks in the Banded series, unless it is proposed that all of these olivine-bearing rocks have been preferentially invaded by a Cl-rich fluid. Boudreau (1988) does suggest a hydrothermal-magmatic origin for the olivine in the rocks near both the J-M Reef and the Picket Pin zone. However, the Cl-rich nature of the apatite in the multiphase inclusions within the plagioclase in AN II and Olivine-bearing zone III is probably not the result of late-stage Cl-rich fluids because the inclusion apatite

Table 4. P and light REE contents (ppm) of plagioclase separates

Sample number	Zone	Rock type[a]	P	La	Ce	Sm	Eu	$(Ce/Sm)_n$
82DCM14	OB V	pc	20	1.40	2.00	0.178	0.351	2.72
82PPC2	OB V	poc	18	0.64	1.10	0.098	0.260	2.71
81CMC4	AN II	pc	16	0.95	1.30	0.120	0.355	2.62
81CMC5	AN II	pc	29	0.79	1.30	0.100	0.359	3.14
81CMC7	AN II	pc	23	0.95	1.70	0.120	0.390	3.42
81CMC9	AN II	pc	24	0.98	1.50	0.130	0.378	2.79
81CMC10	AN II	pc	19	0.83	1.40	0.110	0.392	3.08
81CMC11	AN II	pc	30	0.92	1.30	0.130	0.355	2.42
81CMC12	AN II	pc	21	0.97	1.50	0.140	0.343	2.59
81CMC14	AN II	pc	20	0.62	0.98	0.084	0.294	2.82
82DCM11	AN II	pc	20	0.54	0.48	0.047	0.122	2.47
82PPC3	AN II	pc	20	1.17	2.13	0.172	0.330	2.99
82PPC4	AN II	pc	12	0.52	0.79	0.067	0.240	2.85
82PPC5	AN II	pc	13	0.92	1.70	0.111	0.340	3.70
82PPC6	AN II	pc	15	1.44	2.40	0.210	0.390	2.76
82PPC7	AN II	pc	14	0.87	1.40	0.140	0.310	2.42
82PPC8	AN II	pc	13	1.11	1.80	0.144	0.360	3.02
82PPC9	AN II	pc	22	0.81	1.30	0.092	0.310	3.41
82PPC10	AN II	pc	28	0.66	1.40	0.110	0.090	3.08
82PPC11	AN II	pc	23	0.84	1.30	0.122	0.300	2.57
81CMC1	OB IV	poc	16	1.60	2.70	0.160	0.349	4.08
82DCM8	OB IV	pac	28	1.16	0.60	0.080	0.276	4.83
82PPC12	OB IV	pbac	28	0.97	1.50	0.098	0.300	3.70
82PPC13	OB IV	poc	28	0.91	1.40	0.120	0.300	2.82
81CMC25	OB III	poc	19	1.30	2.20	0.210	0.357	2.53
82DCM20	OB III	pac	23	1.21	2.05	0.158	0.316	3.14
81CMC22	AN I	pc	28	1.30	2.17	0.193	0.349	2.72
81CMC23	AN I	pc	26	1.20	2.14	0.196	0.299	2.64
81CMC27	AN I	pc	18	0.87	1.50	0.160	0.295	2.27
82DCM16	AN I	pc	14	0.63	1.00	0.091	0.257	2.66
82DCM19	AN I	pc	25	0.52	0.82	0.069	0.246	2.87
82DCM23	AN I	pc	21	1.00	1.70	0.145	0.319	2.83
82DCM29	AN I	pc	16	0.85	1.40	0.115	0.322	2.94
83CML13	AN I	pc	16	0.60	1.00	0.076	0.280	3.18
83CML14	AN I	pc	15	0.55	1.10	0.087	0.270	3.06
83CML15	AN I	pc	13	0.70	1.20	0.100	0.300	2.90
83CML16	AN I	pc	15	0.63	1.20	0.110	0.280	2.64
83CML18A	AN I	pc	22	1.35	2.46	0.242	0.360	2.46
83CML18B	AN I	pc	15	0.75	1.20	0.110	0.300	2.64
82DCM2	OB II	poc	30	0.90	1.30	0.107	0.258	2.94
82DCM5	OB II	pc	29	0.83	1.20	0.105	0.204	2.76
82DCM18	GN II	pc	19	1.11	1.88	0.150	0.317	3.03
84CML20	N II	pbc	12	1.34	2.34	0.177	0.284	3.19
84CML8	N I	pbc	15	0.64	1.28	0.091	0.195	3.40

[a] p, plagioclase; o, olivine; b, bronzite; a, augite; c, cumulate

would have been isolated from such fluids. A possibility, discussed but not favored by Boudreau and McCallum (1989), is that the Cl- and F-rich apatites might reflect crystallization from two different parental magmas. However, as noted by those workers, the evidence from sills and dikes associated with the Stillwater Complex suggests that no unusually Cl-rich magmas were involved in the formation of the Stillwater Complex. Nevertheless, the Cl-apatite in the multiphase inclusions strongly implies a magmatic rather than post-magmatic origin for the association of Cl-apatite with olivine-bearing rocks.

Cerium contents in the apatite within the inclusions range from 0.0 to 0.3 wt.% Ce_2O_3. The higher Ce contents occur in one of the Cl-rich apatite samples. The other Cl-rich apatite sample and the F-rich apatite typically contain less than 0.1 wt.% Ce_2O_3. MgO contents are generally between 0.01 and 0.1 wt.%, SiO_2 is between 0.3 and 0.5 wt.%, and FeO is between 0.2 and 0.6 wt.%. Except for Ce, these trace element contents are high compared with those of intercumulus apatite from thoughout the Stillwater Complex analyzed by Boudreau and McCallum (1989).

Effect of apatite on the REE geochemistry of plagioclase separates

Despite its low modal abundance, apatite in the inclusions may significantly affect the REE patterns of both

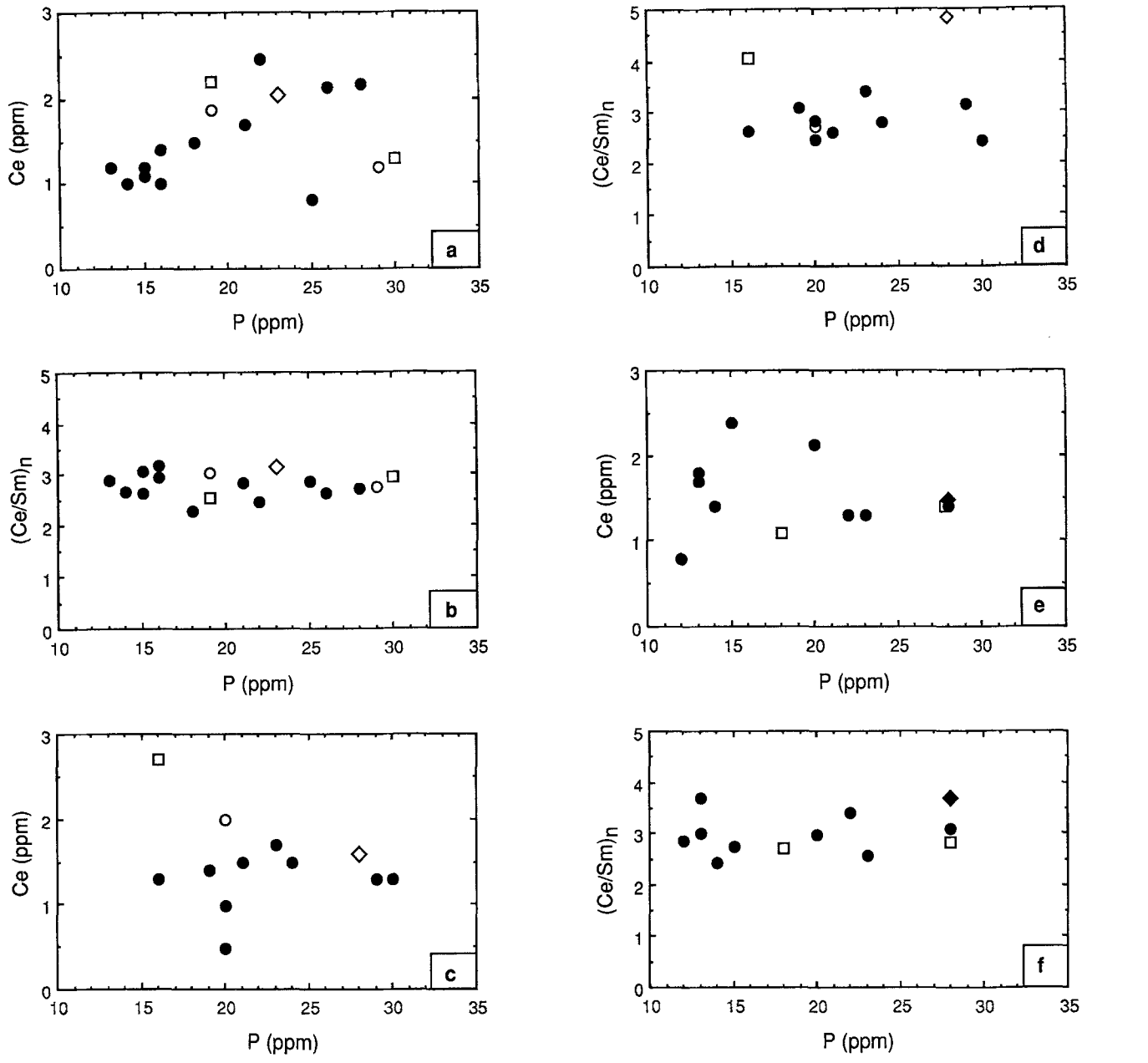

Fig. 7a–f. Plots of P content versus chondrite normalized Ce and (Ce/Sm) for plagioclase separates from three traverses. **a, b** AN I Contact Mountain; **c, d** AN II Contact Mountain; **e, f** AN II Picket Pin Mountain. *Filled circles*, AN I and AN II; *open circles*, anorthosites other than AN I and AN II; *squares*, plagioclase-olivine cumulate; *open diamond*, plagioclase-augite cumulate; *filled diamond*, plagioclase-bronzite cumulate

whole-rocks and plagioclase separates, possibly compromising the usefulness of REE geochemical studies of the anorthosites. This is because the REE mineral-melt partition coefficients for apatite are high, whereas those for plagioclase are very low, except that of Eu^{2+} (Hanson 1980). The potential contamination problem exists regardless of whether apatite was trapped as solid inclusions or whether it crystallized from trapped melt.

The chondrite-normalized REE patterns of plagioclase separates from the Stillwater anorthosites are typical of cumulus plagioclase, having negative slopes and large positive Eu anomalies, and are clearly not dominated by apatite. The problem, however, is to determine whether variations in REE patterns of the plagioclase separates might be caused by variations in the amount of apatite included in plagioclase. On the basis of their REE partition coefficients (Hanson 1980), increasing amounts of apatite would result in decreasing light REE ratios, decreasing Eu anomalies, and increasing REE abundances in plagioclase separates. However, fractionation has exactly the same effects on the REE composition of plagioclase. Therefore, variations in the amount of apatite cannot be detected from the plagioclase REE patterns themselves.

To evaluate the possible REE contribution of the apatite, the plagioclase separates were analyzed for their

P as well as their REE contents as shown in Table 4. (For most samples, the heavy REE were below INAA detection limits.) The P content of the plagioclase separates is low, ranging from 12 to 30 ppm. Plagioclase itself can contain quantities of P within this range (Smith and Brown 1988). The most conservative interpretation, however, is to assume that all of the P in the plagioclase separates is contained in the apatite of the inclusions. Using this assumption, the P contents would reflect the apatite mode in the plagioclase separates. Accordingly, the Ce contents and $(Ce/Sm)_n$ (where n denotes chondrite normalized) are shown plotted against P in Fig. 7a–f for plagioclase separates from three different traverses: one each across AN I and AN II at Contact Mountain and a third across AN II at Picket Pin Mountain. All three data sets include rocks from above and below these two main anorthosite zones. The Ce concentrations show no correlation with P content for either traverse through AN II. With the exception of three samples, the AN I data do show a positive correlation between Ce and P contents. However, this correlation could also be caused by fractionation. In REE modelling studies, REE ratios are of more importance than concentrations. The plots of $(Ce/Sm)_n$ against P contents are therefore more crucial in checking for any effect of apatite. None of the three data sets show any correlation of $(Ce/Sm)_n$ with P content. This is interpreted to indicate that the apatite does not affect the REE signature of the plagioclase because the apatite is present in too small an amount, and/or it contains too small a quantity of REE. It is therefore concluded that the plagioclase separates of the present study can be treated and modelled in REE geochemical studies as pure mineral separates.

Discussion

Origin of the inclusions

The fact that the inclusions are multiphase and that all consist of the same assemblage (implying the same or very similar bulk compositions) argues strongly for their origin as liquid droplets rather than solid aggregates at the time of their entrapment in the plagioclase. The fact that they typically occur within the interior of plagioclase grains and are unrelated to healed fractures is evidence that the inclusions are primary and not secondary.

These inclusions are not comparable to the isolated clinopyroxene, ilmenite, and quartz inclusions reported in plagioclase from massif anorthosites. The isolated inclusions are suggested by some workers (e.g., Smith and Steel 1974) to have formed through solid state exsolution from plagioclase. In contrast, the inclusions in the Stillwater anorthosites are considered magmatic.

The unusual bulk composition of the inclusions precludes their being direct samples of the anorthosite parent liquid. It is also unlikely that they represent trapped residual liquid for the following two reasons. First, most of the inclusions occur within the interiors rather than at the rims of plagioclase grains, implying entrapment at a relatively early stage. Second, calcic plagioclase rims some of the inclusions, whereas relatively sodic plagioclase should crystallize from residual liquid.

The compositions of the phases in the inclusions indicate that they crystallized from a liquid of a peculiar bulk composition. This liquid was calcic, as shown by the compositions of the plagioclase rims, and was enriched in Ti, Mn, REE, P, Zr, Fe, and Mg relative to the bulk of the anorthosites. This suite of elements is the same as the suite known to be partitioned into the mafic fraction of immiscible silicate liquid pairs that form during the fractionation of many basalts (Roedder 1979).

We propose that the inclusions formed from immiscible liquid droplets that exsolved from the parent liquid of the anorthosites. Some of the immiscible droplets became trapped in plagioclase and later crystallized to form the inclusions. Inclusions of the main liquid have not been observed, probably a result of the plagioclase wetting properties of the two liquids.

Liquid immiscibility is a process whereby an originally homogeneous silicate liquid unmixes into two compositionally distinct liquids at some point in its cooling history. It was first found experimentally at geologically reasonable temperatures and compositions in the system leucite-fayalite-silica (Roedder 1951) and was found in natural rocks for the first time in lunar basalts (Roedder and Weiblen 1970). It has since been noted in many terrestrial basalts and andesites as summarized by Roedder (1979). In volcanic rocks, immiscibility typically can be detected petrographically as an emulsion-like mixture of two optically and chemically distinct glasses, with one preserved as globules in the other. This texture has been found in both the mesostasis and in melt inclusions within phenocrysts. Commonly, one glass is colorless and Si-rich, and the other is brown and Fe-rich. Because the two glasses formed as quenched liquids, this texture, with the preserved menisci between the glasses, is the clearest evidence that immiscibility occurred in the liquid state.

Silicate liquid immiscibility has been reported for various bulk compositions, including tholeiitic basalts and andesites (De 1974; Gelinas et al. 1976; Philpotts 1979; Roedder 1979), basaltic komatiites (Ferguson and Currie 1972), high-Al olivine tholeiite (Anderson and Gottfried 1971), and alkali basalts (Philpotts 1976). The timing of liquid immiscibility is variable. In most tholeiitic basalts, it occurs only in the latest stages of fractionation, in very Fe-rich bulk compositions, when there is only about 5% or less liquid remaining. Early immiscibility, however, has been reported and is thought to account for both the ocelli in alkali basalts (Philpotts 1976) and for the varioles in Archean tholeiites (Gelinas et al. 1976). In addition, early immiscibility has been reported to occur in melt inclusions within plagioclase phenocrysts (Philpotts 1981). These examples of early immiscibility are noted because we hypothesize that immiscibility in the Stillwater anorthosites also occurred at a relatively early stage.

Liquid immiscibility is explained in terms of the contrasting melt structures of the two silicate liquids (Hess 1980). One is a highly polymerized tectosilicate (granitic)

melt into which the network-forming cations, Si and Al, as well as the alkalis are partitioned. The other is a relatively depolymerized ferrobasaltic or ferro-pyroxenitic melt into which the network-modifying cations are partitioned. These contrasting melt structures have implications for the nature of the parent liquid of the Stillwater anorthosites. Experimental studies of trace element partitioning between the two immiscible liquids have shown that the ferrobasaltic liquid is enriched in the high charge-density cations, including, in decreasing order of enrichment, P, REE, Ta, Ca, Cr, Ti, Mn, Zr, Mg, Sr, and Ba (Watson 1976; Ryerson and Hess 1978; 1980). Of the suite of trace elements investigated by Watson (1976), only Cs was partitioned into the granitic fraction.

To evaluate whether the Stillwater inclusions could have formed from an immiscible liquid, we calculated their average bulk composition to compare it with compositions of immiscible liquids reported in the literature. The bulk composition of crystalline magmatic inclusions is difficult to estimate, not only because an accurate mode must be determined, but also because the original trapped liquid composition was a combination of the inclusion itself plus some amount of the host phase that crystallized along the inclusions walls after entrapment (Roedder 1984). With this caveat in mind, we calculated the average liquid composition for the inclusions by using visual estimates of the proportions of phases in the inclusions and mineral compositions determined from electron microprobe analyses. To arrive at the mineral proportions and to take into account plagioclase crystallization along the walls of the inclusions, the amounts of ilmenite and apatite in the inclusions were first estimated. Clinopyroxene and plagioclase represented the remainder of each inclusion, and their relative proportions were calculated based on the width of the zoned plagioclase that rimmed the largest inclusions. It was assumed that similar zones were present but too thin to detect around the smaller inclusions. Therefore, 34% plagioclase of An_{90} was included in the calculation of the liquid composition.

The calculated average liquid composition of the inclusions is shown in Table 5, and is plotted on the pseudo-ternary Greig diagram (Fig. 8) along with the compositions and tie-lines of immiscible pairs in some terrestrial and lunar basalts for comparison. The fields of immiscibility (dashed fields) found experimentally in the system leucite-fayalite-silica by Roedder (1951) are also shown. The Stillwater anorthosite inclusion liquid plots within the mafic end of the miscibility gap defined by the other immiscible pairs (Fig. 8).

Table 5. Calculated liquid composition of inclusions

	Average (wt.%)	Standard deviation
SiO_2	43.61	1.80
TiO_2	4.82	1.40
Al_2O_3	13.45	0.94
FeO	9.78	1.10
MnO	0.54	0.17
MgO	7.92	0.33
CaO	18.43	0.41
K_2O	0.02	0.01
Na_2O	0.43	0.07
P_2O_5	0.80	0.49
Total	99.80	

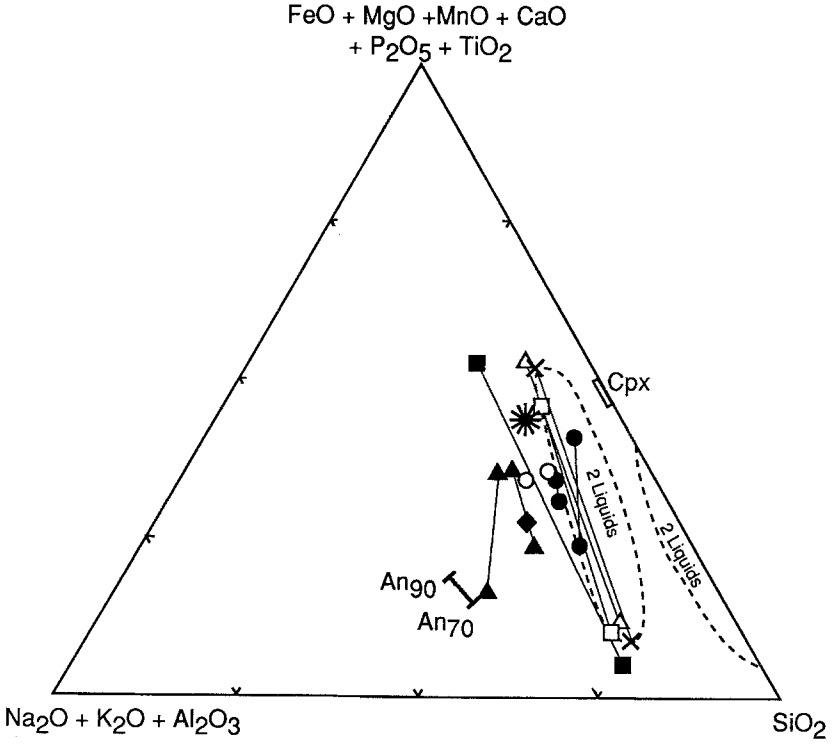

Fig. 8. Pseudo-ternary Greig diagram showing the calculated average composition of the inclusions in the Stillwater anorthosites and representative compositions and tie-lines for immiscible silicate liquid pairs from various basalts. *Star*, calculated Stillwater inclusion liquid, this study; *filled squares*, variole and matrix of Archean tholeiite (Galinas et al. 1976); *filled circles*, ocelli and matrix of Barberton Mountain Land (Transvaal) basaltic komatiites (Ferguson and Currie 1972); *open triangles*, coexisting glasses in melt inclusion in plagioclase phenocrysts (Philpotts 1981); *open squares*, coexisting glasses in lunar basalt (Rutherford et al. 1974); *filled triangles*, ocelli and matrix from alkali basalts (Philpotts 1976); *Xs*, experimentally produced immiscible pair; *open circles*, sills and dikes from the base of the Stillwater Complex (Helz 1985); *filled diamond*, Ao liquid of Irvine et al. (1983); *dashed fields*, fields of liquid immiscibility in the system leucite-fayalite-SiO_2 (Roedder 1951)

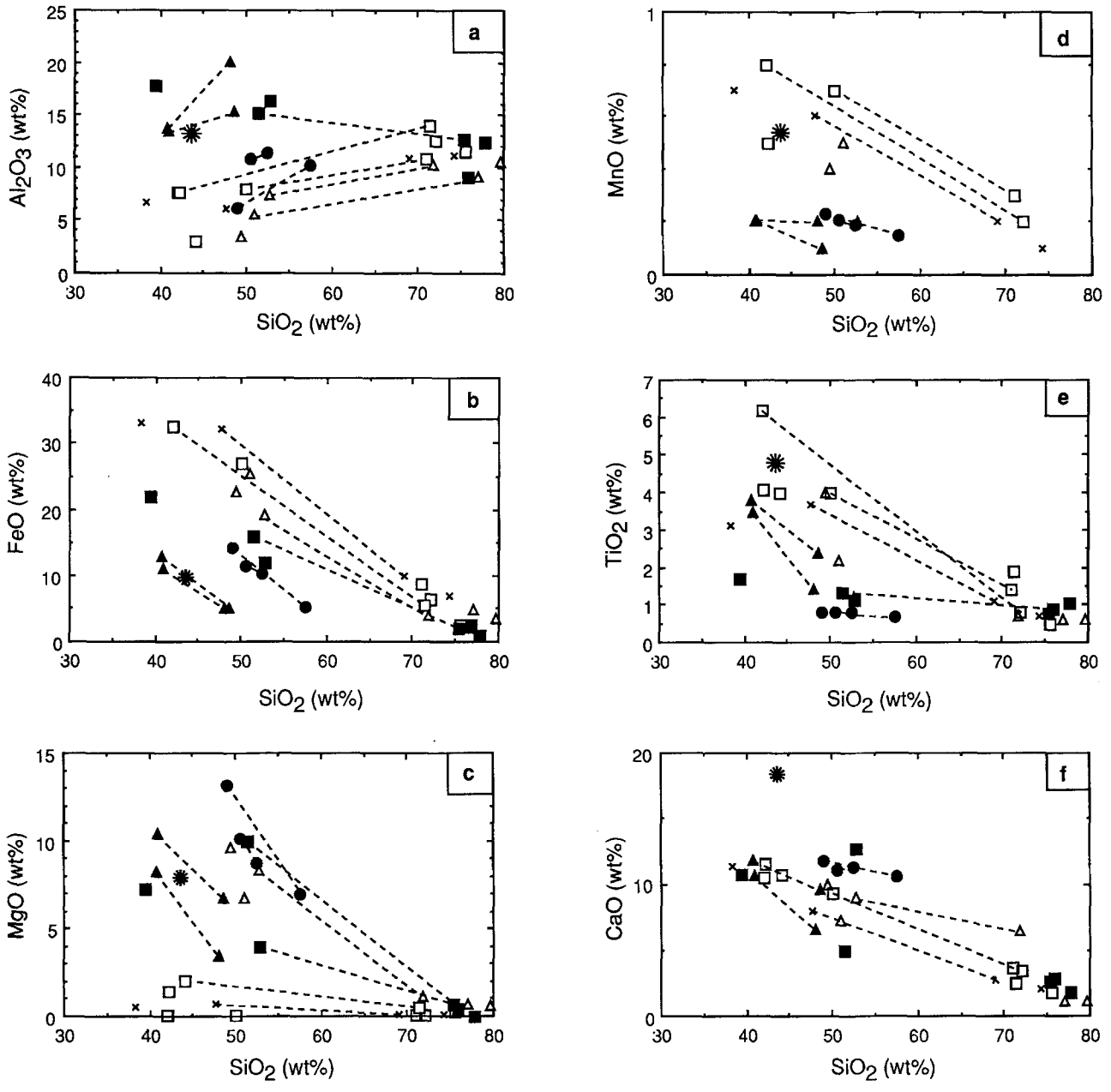

Fig. 9a–f. Plots of SiO_2 against various oxides for immiscible liquid pairs from the literature and the calculated Stillwater anorthosite inclusion liquid. Representative tie-lines for selected pairs are shown, other tie-lines are omitted for clarity. Symbols as in Fig. 8

Although the Greig diagram is useful for showing immiscible liquid compositions, the grouping of elements is also a drawback because liquids of very different compositions can project at the same point on the diagram. Silica variation diagrams are therefore shown in Fig. 9 a–f. Many examples of immiscibility cited in the literature are for tholeiitic residual liquids that are extremely Fe-rich. The Stillwater inclusion liquid is not of this type and its low FeO and high MgO contents are more similar to those of mafic end-members of other types of proposed immiscible pairs reported in the literature. These include rocks having ocellar textures such as Archean tholeiites (Gelinas et al. 1976), basaltic komatiites (Ferguson and Currie 1972), and alkali basalts (Philpotts 1976) as well as immiscible pairs of glasses from melt inclusions in plagioclase phenocrysts (Philpotts 1981). High MgO contents in all of these liquids, including the Stillwater inclusion liquid, are consistent with textural evidence that immiscibility occurred at a relatively early stage in the crystallization history.

The MnO and TiO_2 contents in the calculated inclusion liquid are very similar to the characteristically high contents found in other immiscible mafic end members. Only the high CaO content of the calculated Stillwater inclusion liquid is distinct from the mafic end member of other immiscible pairs (Fig. 9). This is a reflection of the calcic plagioclase and clinopyroxene and is therefore partly an artifact of our calculations. However, it is possible that the Stillwater inclusion liquid was different from other previously reported immiscible pairs be-

cause of an unusually calcic bulk composition of the anorthosite parent liquid.

A second test of liquid immiscibility concerns mineral chemistry. At equilibrium, two immiscible liquids will crystallize the same phases, although in different proportions, and these phases will have the same initial composition in both liquids (Roedder 1979). One test of immiscibility, therefore, is to check that the phases that crystallized from two suspected immiscible liquids have identical compositions. As pointed out by Roedder (1979), the application of this test is difficult at best because it assumes equilibrium and continual exchange of components between the two liquids. We have shown (Figs. 3 and 4) that in the Stillwater anorthosites, the compositions of the inclusion and intercumulus clinopyroxene overlap, as do the compositions of the two types of ilmenite. The areas of compositional overlap could represent the original compositions, indicating the same initial compositions for the phases that crystallized from the immiscible liquids in the anorthosites. However, two potential problems with the mineral chemistry test are as follows. First, the relative timing of crystallization of the intercumulus and inclusion phases in the anorthosites is not known. Second, and more importantly, although the activities for all components must initially be the same in both liquids, the final compositions of the phases will not necessarily be identical. If the immiscible liquids are separated the activities of their components can change independently and the compositions of crystals forming in each may diverge. Such compositional divergence could have occurred when the immiscible droplets became completely isolated in the plagioclase host. This may be the origin of the calcic plagioclase that rims the inclusions.

Implications for the origin of the anorthosites

If the inclusions did form from immiscible liquid droplets as hypothesized, then this has implications for the parent liquid of the anorthosites. The two immiscible liquids in the Stillwater anorthosites were probably analogous to other immiscible pairs in terms of their melt structures: one was polymerized and the other, depolymerized. The depolymerized liquid is represented by the inclusions. We suggest that the polymerized liquid was far more voluminous, but, rather than having the typical granitic composition of many other two-liquid pairs, was high in normative plagioclase content and approached an anorthositic composition. Not all "Si-rich" endmembers of other immiscible pairs are granitic. For example, in the alkali basalts and the basaltic komatiites the Si-rich liquid contains as little as 48.6 wt.% SiO_2 (Fig. 9). We further suggest that the highly polymerized aluminosilicate melt was the main parent liquid of the anorthosites from which the bulk of the plagioclase and the intercumulus phases crystallized.

There are no experimental studies that would be useful in constraining the location on the Greig diagram of the hypothesized miscibility gap encountered by the anorthosites. We can offer the following observation, however. Only a small quantity of the mafic immiscible liquid was produced in the anorthosites, as no evidence has been found for any rocks that may have crystallized from this immiscible liquid. This indicates that the miscibility gap was encountered near the anorthositic limb.

Another possibility for the immiscibility within the anorthosites is that, rather than occurring pervasively throughout the liquid, it occurred only very locally at the margins of crystallizing plagioclase grains within compositional boundary layers. As was observed in an experimental study on the crystallization of a lunar basalt, local fractionation can cause the liquid in the boundary layers around plagioclase grains to split into two liquids while the main body of liquid does not split (Rutherford et al. 1974). Also, in an experimental study of the crystallization of natural tholeiitic basalts, Philpotts (1978) found that the first immiscible globules to form on cooling were Fe rich. The globules nucleated on the surfaces of growing plagioclase laths. On cooling, additional Fe-rich globules formed throughout the residual liquid, but the early ones that formed on plagioclase continued to grow and remained the largest. With further cooling, the immiscible globules were trapped in plagioclase grains and crystallized to form inclusions of pyroxene and minor amounts of opaque oxide. Such a process might account for the multiphase inclusions in the Stillwater anorthosites.

A potential problem with boundary layer immiscibility for the anorthosites is that the large size of some of the inclusions would require compositional boundary layers tens of micrometers thick around plagioclase grains. One prerequisite for the development of substantial compositional boundary layers is that the rate of crystal growth must be more rapid than the rate of diffusion (Bacon 1989). This is unlikely in slowly cooled rocks such as the Stillwater anorthosites. Studies of plagioclase phenocrysts in basaltic liquids reveal boundary layers typically less than 5 μm thick (Bottinga et al. 1966; Muncill and Lasaga 1987). However, the width of compositional boundary layers increases not only with cooling rate, but also with melt viscosity and with the amount of a particular phase crystallizing (Roedder 1984). Therefore, crystallization of large quantities of plagioclase from a viscous polymerized melt could potentially result in a boundary layers of substantial thickness around plagioclase grains, and the immiscibility could have occurred within these boundary layers.

We hypothesize that zones of polymerized melt existed in the Stillwater magma chamber and that AN I and AN II as well as some of the other rocks in the Middle Banded series crystallized from these zones. Evidence that such a liquid might be formed in layered intrusions comes from two sources. First, in studies of the Kilauea Iki lava lake, Helz et al. (1989) found geochemical evidence for the diapiric transfer of low-density melt from the lower to the upper part of the lava lake. The low-density melt was hypothesized to have moved upward in thin finger-like diapirs, and the transfer occurred rapidly enough that the diapirs did not mix with the surrounding melt during transit. In the lava lake, this low-density melt did not form a separate layer; rath-

er it mixed with the crystal+liquid suspension below the roof of the chamber. However, Helz et al. (1989) note that diapiric melt transfer might occur in large intrusions such as the Stillwater Complex, thus producing a low-density, plagioclase-rich melt within the magma chamber. Second, metallurgical studies of the solidification of alloys have focused on the physical processes that occur during crystallization in the crystal+liquid mush zone. These studies have shown that, during solidification, buoyant rejected solute streams out of the mush zone in thin pipes and channels and is expelled upward into the overlying liquid in plumes (Hellawell 1987). Polymerized melt could have been concentrated in the Stillwater magma chamber by such processes.

Crystallization from polymerized melt may account for the distinctive coarse-grained texture of the anorthosites. Based on the positive correlation between the degree of polymerization and melt viscosity (Scarfe and Cronin 1986), the polymerized liquid would have been more viscous than the rest of the liquid in the Stillwater magma chamber. Experimental studies have shown that, with increased melt viscosity, the nucleation density tends to decrease for a given degree of supercooling (Lofgren 1980). Therefore, the coarse grain size of AN I and AN II may be the result of a low nucleation density caused by crystallization from a relatively viscous melt.

The complex plagioclase zoning in AN I and AN II may also be the result of crystallization from polymerized melt. Previous workers have hypothesized that the plagioclase zoning in the anorthosites was the result of extensive circulation of plagioclase grains through different temperature regimes of the magma chamber. However, if the zoning were due to $P-T$ changes during crystallization, then plagioclase grains should have zoning patterns that resemble their nearby neighbors. The fact that zoning patterns do not match up from grain to grain in a single thin section (Czamanske and Scheidle 1985) suggests that the zoning was caused by factors other than $P-T$ changes. Diffusion-controlled growth from a viscous polymerized melt may account for the plagioclase zoning in AN I and AN II.

Czamanske and Bohlen (1990) proposed than AN I and AN II formed as discrete sill-like intrusions of plagioclase-rich crystal mushes that were generated in a deep staging chamber and followed a pathway that repetitively entered the Stillwater magma chamber. However, various observations indicate that AN I and AN II are an integral part, rather than separate from, the rest of the Middle Banded series. This argues against a discrete origin of these thick anorthosites. For example, much of the Middle Banded series is plagioclase rich (Fig. 1). There are numerous thin anorthosite layers as well as the 100-m thick anorthosite in Olivine-bearing zone IV. Many of the rocks in Olivine-bearing zones III and IV have anomalously low cumulus olivine contents of 1 to 10%, compared with cotectic proportions as predicted from appropriate phase diagrams of 15 to 30% (McCallum et al. 1980). Thus, many of these rocks are anorthositic, implying a relationship between their origin and the origin of AN I and AN II. In fact, it is the entire Middle Banded series that is unique compared with much of the Stillwater Complex. AN I and AN II are separated by rocks that (1) have a high proportion of cumulus clinopyroxene relative to orthopyroxene (Fig. 1), as first noted by Hess (1960), in distinct and striking contrast to rocks in the rest of the Stillwater Complex, (2) contain cumulus Mg-rich olivine after its absence for approximately 1000 stratigraphic meters, and (3) display a crystallization sequence different from that of most of the underlying part of the Stillwater Complex (Raedeke and McCallum 1980), with the possible exception of part of Olivine-bearing zone I.

In contrast to a discrete origin as sill-like intrusions, the following observations imply a common origin for AN I and AN II and at least some of the other rocks in the Middle Banded series.

1. The multiphase inclusions of the present study occur in rocks throughout the Middle Banded series, not just in AN I and AN II.
2. Our petrographic study shows that textural features previously reported to be unique to AN I and AN II also occur in Olivine-bearing zones III and IV. These cumulus-olivine-bearing rocks contain notably coarse-grained and nonlaminated plagioclase, textures that are nearly identical to those of AN I and AN II, implying a common origin. This texture is in striking contrast to that of our samples from the Upper and Lower Banded series, including samples from thin anorthosite layers, in which the plagioclase is distinctly finer grained and commonly shows laminations.
3. Plagioclase compositions are virtually constant across the Middle Banded series (Raedeke and McCallum 1980), a feature difficult to explain, but nevertheless implying a common origin for many of the rocks in the Middle Banded series.
4. Evaluation of REE geochemistry of plagioclase separates shows that AN I and AN II are not unique, but instead are geochemically similar to some of the other plagioclase-rich rocks throughout the Lower, Middle, and Upper Banded series (Loferski and Arculus 1991).

Based on these lines of evidence, therefore, we believe it unlikely that AN I and AN II formed as discrete sill-like intrusions of crystal-rich mush and prefer a model whereby they formed within the magma chamber from polymerized melt.

The fact that the multiphase inclusions described here have thus far only been observed in plagioclase from the Middle Banded series is noteworthy and may indicate the presence of polymerized liquids at various horizons throughout the Middle Banded series.

Conclusions

The clinopyroxene+ilmenite+apatite inclusions in the plagioclase from the Stillwater anorthosites are hypothesized to have formed from droplets of immiscible liquid that exsolved from the main liquid giving rise to crystallization of the anorthosites. The immiscibility could either have occurred locally in compositional boundary layers around crystallizing plagioclase grains, or it could have occurred pervasively throughout the parent melt. Analo-

gy to the melt structures of immiscible liquid pairs reported in the literature implies that the parent liquid was a highly polymerized aluminosilicate melt. Crystallization of the anorthosites from such a polymerized melt may account for distinctive features of the anorthosites, such as their coarse grain size and complex plagioclase zoning.

The processes that form nearly monomineralic rocks such as the Stillwater anorthosites are not well understood. Hypotheses typically involve the physical concentration of plagioclase from a basaltic melt followed by the expulsion of intercumulus liquids by various mechanisms. We suggest that processes in the liquid prior to crystallization might be of greater importance. Specifically, we suggest that the liquid in the magma chamber became compositionally stratified and that the anorthosites formed from regions that contained layers of polymerized aluminosilicate liquid enriched in plagioclase components.

The ultimate origin of the polymerized melt cannot be deduced solely on the basis of data from the multiphase inclusions, but previous hypotheses include concentration of felsic rejected solute expelled from underlying parts of the complex and intrusion of a highly aluminous melt followed by double diffusive convection.

Regardless of the origin of the inclusions, the fact remains that REE-bearing apatite occurs within cumulus plagioclase in the Middle Banded series. Our analysis shows that the apatite is not present in amounts large enough to significantly affect the REE geochemistry of the anorthosites. However, as similar inclusions might be present elsewhere in the complex, caution should be used when attempting to use REE geochemistry to model processes in the parent liquid or to look for evidence of multiple parent liquids in the Stillwater Complex.

Acknowledgements. We are grateful to Gerry Czamanske for help in the field, and, along with Diana Scheidle, for providing plagioclase separates and thin sections. We also thank H. Belkin, R. Helz, A. Boudreau and H.R. Naslund for reviewing and improving various drafts of this manuscript.

References

Anderson AT, Gottfried D (1971) Contrasting behavior of P, Ti, and Nb in a differentiated high-alumina olivine-tholeiite and a calc-alkaline andesite suite. Geol Soc Am Bull 82:1929–1942

Bacon CR (1989) Crystallization of accessory phases in magmas by local saturation adjacent to phenocrysts. Geochim Cosmochim Acta 53:1055–1066

Bacon CR, Hirschmann MM (1988) Mg/Mn partitioning as a test for equilibrium between coexisting Fe–Ti oxides. Am Mineral 73:57–61

Bence AE, Albee AL (1968) Empirical correction factors for the electron microprobe analysis of silicates and oxides. J Geol 76:382–403

Bottinga Y, Kudo A, Weill D (1966) Some observations on oscillatory zoning and crystallization of magmatic plagioclase. Am Mineral 51:792–806

Boudreau AE (1986) The role of fluids in the petrogenesis of platinum-group element deposits in the Stillwater Complex, Montana. University of Washington, Seattle, PhD Thesis

Boudreau AE (1988) Investigations of the Stillwater Complex: Part IV. The role of volatiles in the petrogenesis of the J-M Reef, Minneapolis adit section. Can Mineral 26:193–208

Boudreau AE, McCallum IS (1986) Investigations of the Stillwater Complex: Part III. The Picket Pin Pt/Pd deposit. Econ Geol 81:1953–1975

Boudreau AE, McCallum IS (1989) Investigations of the Stillwater Complex: Part V. Apatites as indicators of evolving fluid compositions. Contrib Mineral Petrol 102:138–153

Boudreau AE, Mathez EA, McCallum IS (1986) Halogen geochemistry of the Stillwater and Bushveld complexes: evidence for transport of the platinum-group elements by Cl-rich fluids. J Petrol 27:967–986

Czamanske GK, Bohlen SR (1990) The Stillwater Complex and its anorthosites: an accident of magmatic underplating? Am Mineral 75:37–45

Czamanske GK, Scheidle DA (1985) Characteristics of the Banded-series anorthosites. In: Czamanske GK, Zientek ML (eds) The Stillwater Complex, Montana: geology and guide. Montana Bureau Mines and Geol Spec Pub 92:334–345

Czamanske GK, Zientek ML, eds (1985) The Stillwater Complex, Montana: geology and guide. Montana Bureau Mines and Geol Spec Pub 92

De A (1974) Silicate liquid immiscibility in the Deccan Traps and its petrogenetic significance. Geol Soc Am Bull 85:471–474

Ferguson J, Currie KL (1972) Silicate immiscibility in the ancient "basalts" of the Barberton Mountain Land, Transvaal. Nature, Phys Sci 235:86–89

Foose MP (1985) Primary structural and stratigraphic relations in Banded-series cumulates exposed in the East Boulder Plateau-Contact Mountain area. In: Czamanske GK, Zientek ML (eds) The Stillwater Complex, Montana: geology and guide. Montana Bureau Mines and Geol Spec Pub 92:305–324

Gelinas L, Brooks C, Trzcienski WE, Jr (1976) Archean variolites-quenched immiscible liquids. Can J Earth Sci 13:210–230

Hanson GH (1980) Rare earth elements in petrogenetic studies of igneous systems. Ann Rev Earth Planet Sci 8:371–406

Haskin LA, Salpas PA (1992) Genesis of compositional characteristics of Stillwater AN-I and AN-II thick anorthosite units. Geochim Cosmochim Acta 56:1187–1212

Hellawell A (1987) Local convective flows in partly solidified alloys. In: Loper DE (ed) Structure and dynamics of partly solidified systems. Martinus Nijoff, Boston: pp 5–22

Helz RT (1985) Compositions of fine-grained mafic rocks from sills and dikes associated with the Stillwater complex. In: Czamanske GK, Zientek ML (eds) The Stillwater Complex, Montana: geology and guide. Montana Bureau Mines and Geol Spec Pub 92:97–117

Helz RT, Kirschenbaum H, Marinenko JW (1989) Diapiric transfer of melt in Kilauea Iki lava lake, Hawaii: a quick, efficient process of igneous differentiation. Geol Soc Am Bull 101:578–594

Hess HH (1960) Stillwater igneous complex, Montana – a quantitative mineralogical study. Geol Soc Am Mem 80 p 230

Hess PC (1980) Polymerization model for silicate melts. In: Hargraves RB (ed) Physics of magmatic processes. Princeton University Press, Princeton NJ pp 3–48

Irvine TN (1975) Olivine-pyroxene-plagioclase relations in the system $Mg_2SiO_4-CaAl_2Si_2O_8-KAlSi_3O_8-SiO_2$ and their bearing on the differentiation of stratiform intrusions. Carnegie Inst Washington, Year Book 74:492–500

Irvine TN, Keith DW, Todd SG (1983) The J-M platinum-palladium Reef of the Stillwater Complex, Montana: II. Origin by double-diffusive convective magma mixing and implications for the Bushveld Complex. Econ Geol 78:1287–1334

Kersting AB, Arculus RJ, Delano JW, Loureire D (1989) Electrochemical measurements bearing on the oxidation state of the Skaergaard layered intrusion. Contrib Mineral Petrol 102:376–388

Lindsley DH (1983) Pyroxene thermometry. Am Mineral 68:477–493

Loferski PJ, Arculus RJ (1991) Rare earth element geochemistry of the Banded series of the Stillwater Complex, Montana and its anorthosites: Trans AGU 72:305

Lofgren GE (1980) Experimental studies on the dynamic crystallization of silicate melts. In: Hargraves RB (ed) Physics of magmatic processes. Princeton University Press, Princeton NJ pp 487–551

McCallum IS, Raedeke LD, Mathez EA (1980) Investigations of the Stillwater Complex: Part I. Stratigraphy and structure of the Banded zone. Am J Sci 280-A:59–87

Morse SA (1980) Kiglapait mineralogy II: Fe–Ti oxide minerals and the activities of oxygen and silica. J Petrol 21:685–719

Muncill GE, Lasaga AC (1987) Crystal-growth kinetics of plagioclase in igneous systems: one-atmosphere experiments and application of a simplified growth model. Am Mineral 72:299–312

Nash WP (1984) Phosphate minerals in terrestrial igneous and metamorphic rocks. In: Nriagu JO, Moore PB (eds) Phosphate minerals, pp 215–241

Naslund HR (1987) Lamellae of baddeleyite and Fe–Cr-spinel in ilmenite from the Basistoppen Sill, East Greenland. Can Mineral 25:91–96

Pasteris JD (1985) Relationships between temperature and oxygen fugacity among Fe–Ti oxides in two regions of the Duluth Complex. Can Mineral 23:111–127

Philpotts AR (1976) Silicate liquid immiscibility: its probable extent and petrogenetic significance. Am J Sci 276:1147–1177

Philpotts AR (1978) Textural evidence for liquid immiscibility in tholeiites. Mineral Mag 42:417–425

Philpotts AR (1979) Silicate liquid immiscibility in tholeiitic basalts. J Petrol 20:99–188

Philpotts AR (1981) Liquid immiscibility in silicate melt inclusions in plagioclase phenocrysts. Bull Mineral 104:317–324

Premo WR, Helz RT, Zientek ML, Langston RB (1990) U–Pb and Sm–Nd ages for the Stillwater Complex and its associated sills and dikes, Beartooth Mountains, Montana: identification of a parent magma? Geology 18:1065–1068

Raedeke LD (1982) Petrogenesis of the Stillwater Complex. University of Washington, Seattle, PhD Thesis

Raedeke LD, McCallum IS (1980) A comparison of fractionation trends in the lunar crust and the Stillwater Complex. In: Merrill RB, Papike JJ (eds) Geochim Cosmochim Acta Suppl 12:133–153

Reynolds IM (1985) Contrasted mineralogy and textural relationships in the uppermost titaniferous magnetite layers of the Bushveld Complex in the Beirkaal area north of Rustenburg. Econ Geol 80:1027–1048

Roedder E (1951) Low temperature liquid immiscibility in the system $K_2O-FeO-Al_2O_3-SiO_2$. Am Mineral 35:282–286

Roedder E (1979) Silicate liquid immiscibility in magmas. In: Yoder HS Jr (ed) The evolution of the igneous rocks: fiftieth anniversary perspectives. Princeton University Press, Princeton, NJ p 15–19

Roedder E (1984) Fluid inclusions. In: Ribbe P (ed) Reviews in Mineralogy, vol 12. Mineral Soc Am p 644

Roedder E, Weiblen PW (1970) Silicate liquid immiscibility in lunar magmas, evidence by melt inclusions in lunar rocks. Science 10:641–644

Rutherford MJ, Hess PC, Daniel GH (1974) Experimental liquid line of descent and liquid immiscibility for basalt 70017. Proc 5th Lunar Conf, Suppl 5 Geochim Cosmochim Acta 1:569–583

Ryerson FJ, Hess PC (1978) Implications of liquid-liquid distribution coefficients to mineral-liquid partitioning. Geochim Cosmochim Acta 42:921–932

Ryerson FJ, Hess PC (1980) The role of P_2O_5 in silicate melts. Geochim Cosmochim Acta 64:611–624

Salpas PA, Haskin LA, McCallum IS (1983) Stillwater anorthosites: a lunar analog? Proc 14th Lunar Planet Sci Conf, J Geophys Res 88:B27–B39

Scarfe CM, Cronin DJ (1986) Viscosity-temperature relationships of melts at 1 atm in the system diopside-albite. Am Mineral 71:767–771

Scheidle DA (1983) Plagioclase zoning and compositional variations in Anorthosite I and II along the Contact Mountain traverse, Stillwater Complex, Montana. Stanford University, MS Thesis (unpubl)

Scofield N, Roggenthen WM (1986) Fe–Ti oxide and sulfide mineralogy of the Glen Mountains Layered Complex, Wichita Mountains. In: Gilbert MC (ed) Petrology of the Cambrian Wichita Mountains igneous suite. Oklahoma Geol Surv Guidebook 23:60–64

Smith JV, Brown WL (1988) Feldspar minerals: 1. Crystal structures, physical, chemical, and microstructural properties (2nd edn). Springer, Berlin Heidelberg New York

Smith JV, Steel IM (1974) Intergrowths in lunar and terrestrial anorthosites with implications for lunar differentiation. Am Mineral 59:673–680

Terry RD, Chillenger GV (1955) Summary of "Concerning some additional aids in studying sedimentary formations by M.S. Shvetsov." J Sediment Petrol 25:229–334

Todd SG, Keith DW, Le Roy LW, Schissel DJ, Mann EL, Irvine TN (1982) The J-M platinum-palladium Reef of the Stillwater Complex, Montana: I. Stratigraphy and petrology. Econ Geol 77:1454–1480

Wager LR, Brown GM (1968) Layered igneous rocks. Oliver and Boyd, Edinburgh

Watson EB (1976) Two-liquid partition coefficients: experimental and geochemical implications. Contrib Mineral Petrol 54:119–134

Zientek ML, Czamanske GK, Irvine TN (1985) Stratigraphy and nomenclature for the Stillwater Complex. In: Czamanske GK, Zientek ML (eds) The Stillwater Complex, Montana: geology and guide. Montana Bureau Mines and Geol Spec Pub 92:21–32

Editorial responsibility: J. Ferry